Alpha decay of ^{16}O excited states

Marius Grigorescu,[(1),*] B. Alex Brown,[(1)] and Ovidiu Dumitrescu[(1,2,3),*]

[(1)] *National Superconducting Cyclotron Laboratory and Department of Physics and Astronomy, Michigan State University, East Lansing, Michigan 48824-1321*

[(2)] *Institut de Physique Nucléaire, Division de Physique Théorique, Laboratoire associe au Centré Natíonal de la Recherche Scientifique, Universite Paris-Sud, F-91406 Orsay Cedex, France*

[(3)] *Institut des Sciences Nucléaire, Universite Joseph Fourier, F-38026 Grenoble Cedex, France*

(Received 8 March 1993)

The one-level R-matrix approach is used to calculate alpha decay widths for several low-lying 0^+, 2^+, and 4^+ excited states of the ^{16}O nucleus. The interior wave functions are calculated within the ZBM $(p_{1/2},d_{5/2},s_{1/2})$ shell-model space with various effective interactions. The exterior wave functions are calculated from an α+^{12}C folding model potential obtained with the M3Y interaction. A new method for calculating the channel radius using the matching of the interior and exterior wave functions in the α-decay channel is presented.

PACS number(s): 21.60.Cs, 23.60.+e

I. INTRODUCTION

The theoretical study of α decay has provided a basic test for our understanding of several fundamental quantum phenomena, such as tunneling through the potential barrier, the clusterization process [1], and weak interaction models [2]. However, in spite of the effort invested, a detailed description of the α-particle emission is not yet available.

By contrast to the case of γ or β decay, where the changes in the nuclear structure are small and may be treated within perturbation theory, α decay represents the simplest case of a series including phenomena like the heavy cluster decays and fission, when the transition has dramatic effects, generating in fact two new nuclei. For the calculation of the decay rate, an alternative to the Fermi's Golden Rule in this case was provided by the semiclassical approximation, or later on by the R-matrix theory of nuclear reactions [3]. Following the original description of Gamow, within this theory the α decay assumes two stages, consisting of the process of preformation (structure part), and the process of penetration through the barrier (reaction part) [4, 5]. The microscopic description of preformation has a key role in the understanding of the decay process and requires a precise knowledge of the initial quantum state. To achieve this purpose the shell-model description has been continuously improved considering the correct treatment of Pauli effects [6], of the proton-neutron interaction [7], or extending the space with cluster wave functions [8, 9].

In the present work the α-decay widths of some ^{16}O excited states will be calculated using the R-matrix formalism, with the shell-model wave functions given by three different interactions, ZBM-II [10], Z (ZWM) [11], and REWIL [12]. The model space considered (ZBM) is restrictive, including the last occupied level of ^{16}O, $0p_{1/2}$ and the next two levels $0d_{5/2}$, $1s_{1/2}$ above the shell closure at $N = Z = 8$. However, the present calculation accounts for all possible configurations within this model space. The structure of ^{16}O assumed here consists of an inert ^{12}C core, and four active nucleons. In the α decay these four nucleons are emitted, and the calculation of the widths provides a natural test of the effective interactions employed.

The ^{12}C-α scattering wave functions will be generated by the Coulomb potential plus the realistic M3Y double folding potential [13], in which one uses an effective interaction derived from the G-matrix elements based on the Reid soft-core NN potential [14] in the form assuming only a one-pion exchange potential (OPEP) force between the states with odd relative angular momentum [15].

The next section contains a detailed presentation of these calculations. The main parameter of the R-matrix approach, the channel radius, will be chosen both according to the previous suggestions [16, 17] as well as by a new procedure which eliminates to a large extent the ambiguities of matching the internal and scattering radial wave functions in the ^{12}C+α channel. The results and the main conclusions are summarized in Sec. III.

II. THE DECAY WIDTHS

Within the R-matrix formalism the many-body coordinate space is separated in two regions by a hypersurface S surrounding the origin at the channel radius r_c. For a general α decay $A + 4 \rightarrow A + \alpha$ the coordinates on this surface are the internal coordinates of the fragments $q^A_{\rm int}$, $q^\alpha_{\rm int}$ and the angular coordinates Ω of the relative motion. Thus the surface element is $dS_c = r_c^2 d\Omega dq^\alpha_{\rm int} dq^A_{\rm int}$. On S

*Permanent address: Department of Theoretical Physics, Institute of Physics and Nuclear Engineering, Institute of Atomic Physics, P.O. Box MG-6, Magurele, Bucharest R-76900, Romania.

is defined a complete set of orthonormal functions Φ_c. If the channel radius is infinite, then this set is given by all possible channel spin functions

$$\Phi_c = \psi^{\alpha}_{\rm int}\psi^{A}_{\rm int}\frac{Y_{LM}}{r_c} \tag{1}$$

expressed in terms of the two internal functions of the fragments and the angular wave function of the relative motion. However, this set is assumed to be a reasonable approximation also for finite radii.

In the external region the interaction between the fragments α and A is given by a phenomenological potential, and the radial wave function for the relative motion is a superposition of regular (F) and irregular (G) solutions for this potential scattering problem:

$$\Psi_{\rm ass} = F_L + C_L(G_L + iF_L) \tag{2}$$

with the coefficient $C_L = -\frac{i}{2}(e^{2i\delta_L} - 1)$ expressed in terms of the phase shift angle δ_L. This phase shift depends on the energy, and when $\delta_L(E_r) = \frac{\pi}{2} + m\pi$ there is a resonance. Near the resonance energy E_r the cross section has a Breit-Wigner form and the derivative of the phase shift with respect to the energy is related to the width Γ by the simple formula

$$\frac{2}{\Gamma} = \left.\frac{d\delta_L}{dE}\right|_{E_r}. \tag{3}$$

At resonance the cross section has a maximum, the coefficient $C_L = i$ and thus the wave function behaves asymptotically as the irregular solution for the potential scattering. In our case the ^{12}C-α potential is given by the folding model previously employed in [18]. This is obtained numerically, and then is interpolated by cubic spline functions to improve the accuracy of the numerical integration. The radial scattering wave functions are calculated at the experimental resonance energies using the Numerov algorithm. At a distance of 10 fm the nuclear folding potential V_n has practically no contribution, and the regular solution is normalized to have the asymptotic behavior of the Coulomb functions [19]. The value of the irregular solution at this distance is obtained from the Wronskian relation $F'_L G_L - F_L G'_L = 1$ and then the whole irregular solution is obtained integrating backwards to the origin. However, at small distances the fragments interact strongly, and this asymptotic solution should be gradually replaced by the "internal" wave function supposed to describe the compound system before decay.

In the single-channel approximation the internal function is assumed to be a regular eigenfunction X of the model Hamiltonian H,

$$HX = E_X X \tag{4}$$

normed in the volume surrounded by S and determined such that [3]

$$\int dS\Phi^*_c \bigtriangledown_{\rm norm}(r_c X) = B_c \int dS\Phi^*_c X \tag{5}$$

with B_c the boundary parameter.

If the fragments would remain distinct in the internal region, then X could be represented as a clusterlike wave function, by an antisymmetrized product between a surface function Φ_c and a radial function $f_{\rm int}$ for the relative distance. But as the fragments lose their identity, $f_{\rm int}$ corresponding to the cluster component should be extracted from the shell model state X by projection onto the channel c. In terms of a complete orthonormal set R_{NL} the projected function $f_{\rm int}$ will be defined by the sum

$$f_{\rm int}(r) = \sum_N \theta^X_{Nc} r R_{NL}(r, \alpha_r), \tag{6}$$

where $\theta^X_{Nc} = \langle \mathcal{A}(\psi^{\alpha}_{\rm int}\psi^{A}_{\rm int}Y_{LM}R_{NL}) \mid X\rangle$ and $\mathcal{A}$ stands for the antisymmetrization operator. The basis functions R_{NL} are chosen as the radial eigenstates for a particle having the reduced mass $A_{\rm red} = 4A/(4+A)$ placed in a harmonic oscillator potential. The oscillator constant is $\alpha_r = \sqrt{A_{\rm red}}\alpha_0$, with $\alpha_0 = \sqrt{\frac{m_0\omega}{\hbar}}$, m_0 is the nucleon mass, and ω is the oscillator frequency for the shell model potential of the initial nucleus. The radial function $f_{\rm int}$ has a central role in the R-matrix calculation because its square at the channel radius gives the formation probability of the fragments. Using this function, the boundary parameter B_c may be simply estimated as

$$B_c = \rho\left.\frac{(f_{\rm int})'}{f_{\rm int}}\right|_{r_c} \tag{7}$$

with the prime denoting the derivative with respect to $\rho = kr$, $k = \sqrt{2m_0 A_{\rm red}E_{\rm c.m.}}/\hbar$, and $E_{\rm c.m.}$ is the decay energy in the center of mass frame.

The coefficients θ^X_{Nc} are complicated because it is difficult to perform separate integrals over the intrinsic coordinates of the fragments, but it was shown [20] that a simpler form may be obtained assuming that all centers of mass of the nuclei involved in the reaction have a harmonic oscillator motion with the same frequency. In this case the integral defining θ may be expressed in terms of the whole wave function of the nucleus A , instead of the intrinsic one, and introducing further a complete set of four-body shell model wave functions $\mid \Psi_\beta >$ then

$$\begin{aligned}\theta^X_{Nc} = &\left(\frac{A+4}{A}\right)^{N+L/2} \\ &\times \sum_\beta \binom{A}{4}^{1/2} \langle \Psi_A \Psi_\beta \mid\} X\rangle \\ &\times \langle \psi^{\alpha}_{\rm int} R_{NL}(R_\alpha, 2\alpha_0) Y_{LM} \mid \Psi_\beta\rangle.\end{aligned} \tag{8}$$

The intrinsic function of the α particle $\psi^{\alpha}_{\rm int}$ is expressed in terms of harmonic oscillator ground-state wave functions, with the oscillator constant $\beta^2 = 0.702$ fm^{-2} chosen to fit the matter radius [15, 21]. In the present calculation the states X are represented by the shell-model wave functions and correspond to the low-lying excited states of ^{16}O known to decay emitting an α particle. The four-particle coefficients of fractional parentage $\langle \Psi_A \Psi_\beta \mid\} X\rangle$ are obtained by assuming a wave function Ψ_β constructed within the proton-neutron ZBM model space.

The last factor $\langle \psi^{\alpha}_{\rm int} R_{NL}(R_\alpha, 2\alpha_0) Y_{LM}(\Omega_\alpha) \mid \Psi_\beta\rangle$ is calculated by expanding Ψ_β in terms of products of two-

proton and two-neutron single-particle wave functions, the expansion coefficients being a product of two two-particle fractional parentage coefficients [22]. The first factor $(\frac{A+4}{A})^{N+L/2}$ comes from the Moshinski transformation for nonequal masses [23].

In Fig. 1 we see the extent to which the projected radial function $f_{\rm int}$ depends on the model Hamiltonian for the first four 2^+ states of ^{16}O, denoted 2^+_{1-4}, having the measured excitation energies E_X=6.917, 9.844, 11.520, 13.020 MeV, [24]. The lowest excitation 2^+_1 is below the threshold for the α emission (7.16 MeV), but it was also included because of its importance for the study of the parity violating α transitions [18, 25].

When the internal and the external wave functions for the resonance energy are joined at the channel surface, a functional relation appears between the phase shift, the boundary parameter, and the "reduced widths" γ. Therefore the explicit formula for the calculation of the width using this approach is [17]

$$\Gamma = \frac{2}{\frac{P}{\gamma^2}+\frac{P\dot{S}-\dot{P}(S-B)}{P^2+(S-B)^2}-\dot{\phi}}\,|_{r_c}\,. \tag{9}$$

Here the overdots denote the derivative with respect to the energy, $B=\rho G'/G$, $P=\rho/(F^2+G^2)$, $S=P(FF'+GG')$, $\rho=kr$, $\tan\phi=F/G=(S-B)/P$, and

$$\gamma=\sqrt{\frac{\hbar^2 r_c}{2m_0 A_{\rm red}}}\sum_N \theta^X_{Nc} R_{NL}(r_c,\alpha_r). \tag{10}$$

In particular if G has a maximum ($B=0$) at the channel radius and $|\frac{F}{G}|\ll 1$, as is usually the case in the barrier region, this formula takes the simple form

$$\Gamma_0 = 2P\gamma^2. \tag{11}$$

The major difficulty encountered in such a calculation is a strong dependence on the channel radius, with large variations around the nodes of G, where the boundary parameter B becomes infinite and changes sign.

According to the previous suggestions [17,16] the channel radius should be chosen in the region of the last peak of the regular scattering wave function F_L inside the barrier. More precisely Ref. [17] takes the points where F_L decreases to one-half of the peak value (case I) and Ref. [16] takes the point corresponding to the peak (case II). In increasing order, these three values will be denoted in the following by $r_{\rm I}^{\rm min}$, $r_{\rm II}$, $r_{\rm I}^{\rm max}$, and in our case are close to the values 3.6, 4.3, and 5.6 fm used in [25]. The average of the values $r_{\rm II}$ for the transitions 2^+_{2-4} is $r_{\rm II}^{\rm av}=4.24$ fm, and this radius was also used for comparison. To fix a reference for the size range considered, we recall that the experimental rms charge and matter radius of ^{16}O are $\langle r^2\rangle^{1/2}_{\rm ch}=2.71$ fm and $\langle r^2\rangle^{1/2}_{n+p}=2.59$ fm [15, 24, 21].

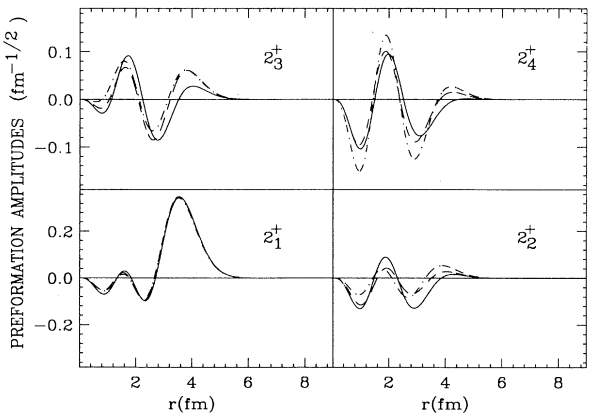

FIG. 1. The radial functions $f_{\rm int}$ projected from 2^+ shell model states. Solid line: REWIL; dashes: Z; Dot-dashed line: ZBM-II.

The antisymmetrization between the α particle and the residual ^{12}C nucleus affects the radial scattering wave functions, changing the function F_L to

$$\tilde{F}_L(r)=F_L(r)-\int_0^\infty dr'\,K_L(r,r')F_L(r'), \tag{12}$$

where K_L is the Pauli kernel [6, 18]. Numerical calculations show that for all the states investigated the corrected function $\tilde{F}_L$ has only one dominant maximum in the internal region, at a radius $r_{\rm kernel}$ very close to $r_{\rm II}$. For small radii $\tilde{F}_L$ almost vanishes, while near the maximum and at larger distances it becomes identical with F_L.

The intrinsic wave function X was generated using three different Hamiltonians: ZBM-II, Z, and REWIL. The interaction ZBM-II was determined from Talmi fits for ^{16}O in the p and sd shells [11], while the Z interaction was constructed using free nucleon-nucleon potentials, with minimal corrections from the experimental energy levels in $A=16$, 17, 18 nuclei [11,12]. REWIL is entirely obtained by a fit of 134 binding and excitation energies of selected levels in $A=13$–22 nuclei, considering the matrix elements of the Hamiltonian as free parameters [12].

The corresponding widths of the states 2^+_{2-4} given by (9) for the various alternatives in the choice of the channel radius and of the interaction are given in Tables I–III. In addition the reduced widths and Γ_0 calculated at the average radius are included for comparison. For the decay energies $E_{\rm c.m.}$ the experimental values were taken, assuming that the shell-model calculation reproduces the correct order of the levels.

Clearly, the variations in the widths determined by different choices of the channel radius or of the interaction are large. In fact, the preformation amplitudes given by the three interactions considered (Fig. 1) come very close for the state 2^+_1 below threshold, while large differences appear for the other states.

The kernel correction to the position of the last maximum is small, showing that the radius range considered is large enough to neglect the antisymmetrization effects on the scattering states, and is appropriate for the choice of the channel surface. However, up to this point precise matching of the internal and scattering wave functions has not been made and therefore the numerical estimates remain to a large extent qualitative.

Further agreement with the data might be expected,

TABLE I. Excitation energies $E^{\rm th}$ (MeV), widths (keV), and the reduced widths γ (MeV$^{1/2}$) for the state 2_2^+. $E_{\rm c.m.}$=2.69 MeV, $r_{\rm I}^{\rm min}$=3.67, $r_{\rm II}$=4.37, $r_{\rm kernel}$=4.38, $r_{\rm I}^{\rm max}$=5.35.

Interaction	$E^{\rm th}$	Γ ($r_{\rm I}^{\rm min}$)	Γ ($r_{\rm II}$)	Γ ($r_{\rm II}^{\rm av}$)	Γ ($r_{\rm Kernel}$)	Γ ($r_{\rm I}^{\rm max}$)	Γ_0 ($r_{\rm II}^{\rm av}$)	γ ($r_{\rm II}^{\rm av}$)
Z	11.86	75.3	1.2	2.2	1.2	6.2×10^{-3}	2.1	3.2×10^{-2}
ZBM-II	10.54	333	3.1	6.2	2.9	1.2×10^{-2}	6	5.4×10^{-2}
REWIL	9.66	141	0.64	0.9	0.61	6.0×10^{-3}	0.9	2.0×10^{-2}

TABLE II. Excitation energies $E^{\rm th}$ (MeV), widths (keV), and the reduced widths γ (MeV$^{1/2}$) for the state 2_3^+. $E_{\rm c.m.}$=4.36 MeV, $r_{\rm I}^{\rm min}$=3.60, $r_{\rm II}$=4.23, $r_{\rm kernel}$=4.22, $r_{\rm I}^{\rm max}$=5.02.

Interaction	$E^{\rm th}$	Γ ($r_{\rm I}^{\rm min}$)	Γ ($r_{\rm II}$)	Γ ($r_{\rm II}^{\rm av}$)	Γ ($r_{\rm Kernel}$)	Γ ($r_{\rm I}^{\rm max}$)	Γ_0 ($r_{\rm II}^{\rm av}$)	γ ($r_{\rm II}^{\rm av}$)
Z	12.86	91	149	131	160	0.53	51	5.8×10^{-2}
ZBM-II	13.27	107	138	122	150	0.46	47.2	5.5×10^{-2}
REWIL	13.32	2.1	46.8	75.4	41.8	0.24	16	3.2×10^{-2}

TABLE III. Excitation energies $E^{\rm th}$ (MeV), widths (keV), and the reduced width γ (MeV$^{1/2}$) for the state 2_4^+. $E_{\rm c.m.}$=5.86 MeV, $r_{\rm I}^{\rm min}$=3.54, $r_{\rm II}$=4.12, $r_{\rm kernel}$=4.12, $r_{\rm I}^{\rm max}$=4.82.

Interaction	$E^{\rm th}$	Γ ($r_{\rm I}^{\rm min}$)	Γ ($r_{\rm II}$)	Γ ($r_{\rm II}^{\rm av}$)	Γ ($r_{\rm Kernel}$)	Γ ($r_{\rm I}^{\rm max}$)	Γ_0 ($r_{\rm II}^{\rm av}$)	γ ($r_{\rm II}^{\rm av}$)
Z	14.11	23.5	138	31.3	145	0.81	6.1	1.9×10^{-2}
ZBM-II	13.54	28.3	474	97.5	499	2.1	18.9	3.4×10^{-2}
REWIL	14.99	80.3	38	1.7	41.2	0.04	0.33	-4.5×10^{-3}

TABLE IV. Excitation energies (MeV), widths (keV), and matching parameters for the states 0_i^+,2_i^+,4_i^+ obtained with the REWIL interaction.

L_i^+	$E^{\rm exp}$	$E^{\rm th}$	$\Gamma_{\rm exp}$	$\Gamma_{\rm th}$	Γ_0	ε	r_c (fm)	$r_f^{\rm max}$ (fm)
0_2^+	11.26	11.6	(2500)?	903	839	5%	3.34	3.34
0_3^+	12.05	14.5	1.5±0.5	96	89.5	−15%	2.44	2.44
0_4^+	14.03	15.9	200±15	26	26	32%	3.79	3.79
2_2^+	9.84	9.66	0.625±0.1	1.1	1	0%	4.1	4.3
2_3^+	11.52	13.32	71±3	38.1	37.4	24.5%	4	4
2_4^+	13.02	14.99	150±10	245	210	14%	3.09	3.09
4_1^+	10.35	11.4	27±3	34.3	46.6	100%	3.43	3.43
4_2^+	11.09	13.3	0.28±0.05	0.7	0.64	0%	3.95	4.07
4_3^+	13.87	14.3	∼49	293	209	29%	3.66	3.66
4_4^+	14.62	16.6	∼389	36.2	31.4	30%	3.63	3.63

if a more precise definition of the channel radius would be available. In fact, we know that in the internal region the relative wave function should be $f_{\rm int}$ rather than F_L, and only near the barrier this becomes inaccurate and must be replaced by the asymptotic solution G_L. Thus it appears natural to fix the channel radius near the last maximum of $f_{\rm int}$ instead of F_L, when both the internal and the scattering wave functions should be accurate, and such that $B_c = B$, namely:

$$\left.\frac{f'_{\rm int}}{f_{\rm int}}\right|_{r_c} = \left.\frac{G'}{G}\right|_{r_c}. \tag{13}$$

When this condition is fulfilled, it becomes possible to extend continuously G_L in the internal region by $f_{\rm int}^{\rm scaled} = \nu f_{\rm int}$, with $\nu = G_L(r_c)/f_{\rm int}(r_c)$.

To solve this problem we adopted the method of fixing the channel radius r_c at the last maximum $r_f^{\rm max}$ of $f_{\rm int}$, ($B_c = 0$), and changing the nuclear folding potential $V_n(r)$ to $(1+\varepsilon)V_n(r)$. The point $r_f^{\rm max}$ was chosen because it corresponds to the peak in the preformation probability which is the furthest from the origin. Apparently it corresponds to the largest decay rate, but this is not always true, as one can see from Table I, where the widths decrease continuously at the increase of the channel radius. In fact the resonant behavior of the global wave function is reflected by the relative amplitudes of the successive maxima and therefore if the internal function is assumed to be correct up to the last maximum, then we may scale its amplitude at this point according to the asymptotic normalization.

Following this matching procedure we calculated the α-decay widths from the low-lying 0^+_{2-4}, 2^+_{2-4}, and 4^+_{1-4} states of ^{16}O obtained using both REWIL and ZBM-II interactions. The widths and the parameters of the REWIL calculation are summarized in Table IV. As an example, the global wave functions resulting from the matching of the internal and scattering states for the 2^+ transitions are presented in Fig. 2. The number of extrema between the origin and the matching point, denoted N_G for G and N_f for $f_{\rm int}$, are the same and is not affected by the potential changes considered. For the transition 2^+_4, the REWIL projected function has the last maximum at 4.75 fm, and its amplitude is very small (Fig. 1). Thus it is more realistic to consider the matching at smaller distances, or even at the next-to-last extremum. The matching outside the maximum (Fig. 2) was achieved by solving Eq. (13) without any potential change, obtaining $r_c = 3.7$ fm and correspondingly a width $\Gamma = 74$ keV. The result of changing the potential and matching at the next-to-last extremum, at 3.09 fm, is 245 keV (see Table IV). We can obtain the matching at $B \neq 0$ by solving (13) near $r_f^{\rm max}$ without any potential change also for the decays of 2^+_2 and 4^+_2 states. However, we observed that in these cases a change in the potential shifting the matching point towards $r_f^{\rm max}$ brings the widths closer to the experimental values. It is interesting to remark that the small width observed for the 2^+_2 transition is correlated with the behavior of the global wave function which appears concentrated in the internal re-

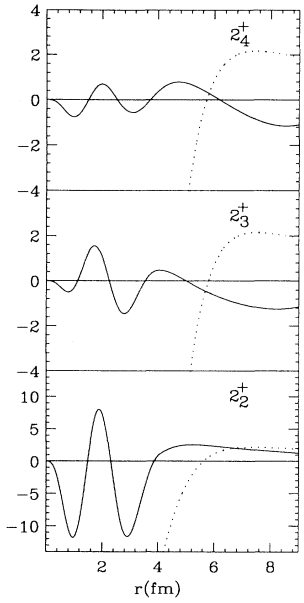

FIG. 2. Solid line: extension from REWIL radial internal functions to scattering states, normalized to have the asymptotic behavior of the Coulomb functions. Dots: the ^{12}C-α potential with the scale in MeV. For the states $2^+_{2,3}$, the matching radius r_c and correction factor ε of the M3Y potential are given in Table IV.

TABLE V. Excitation energies (MeV), widths (keV), and matching parameters for the states 0^+_i,2^+_i,4^+_i obtained with the ZBM-II interaction.

L^+_i	$E^{\rm exp}$	$E^{\rm th}$	$\Gamma_{\rm exp}$	$\Gamma_{\rm th}$	Γ_0	ε	r_c (fm)	$r_f^{\rm max}$ (fm)
0^+_2	11.26	10.73	(2500)?	502	375	13.8%	3.21	3.21
0^+_3	12.05	12.44	1.5±0.5	0.13	0.11	−22%	4.41	4.41
0^+_4	14.03	14.58	200±15	214	212	−5%	3.44	3.44
2^+_2	9.84	10.54	0.625±0.1	6.7	5.3	−30%	3.8	3.89
2^+_3	11.52	13.27	71±3	192	185	−14%	3.79	3.79
2^+_4	13.02	13.54	150±10	23.8	23.6	20%	4.19	4.19
4^+_1	10.35	10.42	27±3	26	32	90%	3.41	3.41
4^+_2	11.09	13.58	0.28±0.05	3.5	3.6	−30%	3.6	3.7
4^+_3	13.87	14.54	∼49	709	487	−8.5%	3.2	3.2
4^+_4	14.62	15.60	∼389	0.06	0.06	−2%	3.14	3.14

gion (Fig. 2). A similar situation was noticed also for the 4_2^+ transition. The results are not strongly influenced by the manner of generating the potential change, because, for example, the addition of a Woods-Saxon term with variable depth has almost the same effect.

One should note that the matching of 4_1^+ wave functions at $B = 0$ requires a large potential change ($\varepsilon \sim 100\%$) (Tables IV and V) and a different number of extrema, $N_G - N_f = 1$. The same situation appears for the 0_4^+ transition calculated with REWIL (Table IV) and 0_3^+ calculated with ZBM-II (Table V). In the case of ZBM-II state 2_3^+, (Table V), we have $N_G - N_f = -1$ but the additional extremum of $f_{\rm int}$ has a very small amplitude. For the ZBM-II states 2_2^+, 4_2^+, the matching at the last maximum would require a large ε and a difference $\Delta_N = \mid N_G - N_f \mid$ of at least 2. However, by increasing N_G the penetrability increases and the width is overestimated. Therefore to obtain a reasonable value it is convenient to allow for a small shift Δ_r in r_c from the maximum if this decreases Δ_N. In the present case of ZBM-II $2_2^+, 4_2^+$ states, for a channel radius close to the $f_f^{\max}$ within $\Delta_r = 0.1$ fm (Table V) it is possible to obtain a solution with Δ_N decreased by one.

The comparison between the excitation energies and the decay widths obtained using REWIL (Table IV) and ZBM-II (Table V) interactions shows that REWIL gives better results for the 2^+ states, ZBM-II for the 0^+ states, while in the case of the 4^+ transitions the quality is almost the same. In both cases the results indicate also a possible level crossing for the couple 4_3^+-4_4^+ with respect to the data.

III. SUMMARY AND CONCLUSION

The α decays from the ^{16}O excited states 2_{2-4}^+ were used to compare three effective Hamiltonians ZBM-II, Z, and REWIL defined within the ZBM shell-model space. The three model Hamiltonians are obtained by different procedures, but are known to give similar results concerning the energy levels and the electromagnetic properties of the light nuclei [12, 26]. This comparison is extended now to the α channel, calculating the radial projected functions and the decay widths. These functions (Fig. 1) have almost the same radial dependence irrespective of interaction, and in the case of REWIL, their last maximum for the 2_{2-4}^+ transitions appears at a larger distance than for ZBM-II or Z. This shift brings this maximum closer to the corresponding one for the scattering states obtained with the unrenormalized folding model potential.

Considering first the previous suggestions in the choice of the channel radius, we showed that a selection around the last maximum of the regular scattering solution gives the widths in a range including the measured values. However, these results (Tables I–III) are mainly qualitative, appearing quite sensitive to the variations of the reduced widths or of the channel radius parameter. For more precise estimates, instead of expressing the width only in terms of the scattering problem we started from the internal projected wave functions $f_{\rm int}$ and attempted to find an appropriate asymptotic extension to the resonance wave functions G. In our case this matching of the wave functions was obtained by fixing the channel radius at the last peak of the internal function ($B_c = 0$) and changing the potential. This change shifts slightly the last maximum of G inside the barrier until it has the same position as the corresponding one for the internal state. The results obtained in the treatment of α decays from the ^{16}O excited states 2_{2-4}^+, 0_{2-4}^+, and 4_{1-4}^+ calculated using the REWIL and ZBM-II interactions are given in Tables IV and V. In the case of REWIL 0^+, $2_{3,4}^+$, and $4_{1,3,4}^+$ excited states the matching was obtained at $B = 0$ by the change of the potential, while for the narrow 2_2^+ and 4_2^+ transitions it was obtained without potential change, at a channel radius outside, but near the maximum, obtained by solving (13). The extensions of radial functions projected from the REWIL 2_{2-4}^+ shell-model states are shown in Fig. 2.

In the case of ZBM-II excited states the matching was obtained by potential change at the last maximum of $f_{\rm int}$, excepting the 2_2^+ and 4_2^+ transitions, when the channel radius is slightly off the maximum.

The calculated widths are in reasonable agreement with experiment, reproducing quite well the variations of several orders of magnitude observed between the decay widths for the low-lying states considered at each angular momentum investigated. The remaining differences may be due to the limitations of the model space, as well as to possible inversions in the level ordering. Enlarging the space will allow the spatial extension of the volume occupied by the internal functions, and therefore a smaller shift between their last maximum and the one observed for the scattering functions might be obtained [8]. Worth noting is that the treatment of the correlations responsible for clusterization and decay is improved not only by the increase of the model space, but also by a complete account of the possible configurations. The simple extension provided by the explicit inclusion of the cluster wave functions [9] in the structure of the initial states seems to diminish the discrepancy between theory and experiment, but should be tested for other processes too in order to be sure whether the additional cluster component does not alter the properties already described within the usual shell model. In our case, the shell-model treatment proves to reproduce a large amount of experimental data in ^{16}O, indicating the relevance of the present attempt to achieve a microscopic description of the α decay.

ACKNOWLEDGMENTS

One of the authors (O.D.) would like to thank Professor G. Bertsch, Professor N. Vinh Mau, Professor H. Flocard, and Professor D. Vautherin for the fruitful discussions. He also would like to express his gratitude to the Michigan State University, National Superconducting Cyclotron Laboratory, East Lansing, Ministere de la Recherche et de la Technologie, France, CIES, Institut de Physique Nucleaire, Orsay, and Institut des Sciences Nucleaires Grenoble for the warm hospitality and for the financial support. He would like to thank the Soros Foundation from Bucharest, Romania for the travel grant used to travel in the United States. This work was supported in part by U.S. National Science Foundation Grant No. PHY-90-17077.

[1] Y. Akaishi, K. Kato, H. Noto, and S. Okabe, *Developments of Nuclear Cluster Dynamics* (World Scientific, Singapore, 1989).
[2] M. Gari, Phys. Rep. C **6**, 317 (1973).
[3] A.M. Lane and R.G. Thomas, Rev. Mod. Phys. **30**, 257 (1958).
[4] H.J. Mang, Ann. Rev. Nucl. Sci. **14**, 1 (1964); Z. Phys. **148**, 572 (1957); Phys. Rev. **119**, 1069 (1960).
[5] O. Dumitrescu, Fiz. Elem. Chastits At. Yadra **10**, 377 (1979) [Sov. J. Part. Nucl. **10**, 147 (1979)].
[6] A. Bulgac, S. Holan, F. Carstoiu, and O. Dumitrescu, Nuovo Cimento A **70**, 142 (1982).
[7] G. Dodig-Crnkovic, F.A. Janouch, and R.J. Liotta, Nucl. Phys. **A501**, 533 (1989).
[8] T. Tomoda and A. Arima, Nucl. Phys. **A303**, 217 (1978).
[9] K. Varga, R.G. Lovas, and R.J. Liotta, Nucl. Phys. **A550**, 421 (1992).
[10] A.P. Zuker, B. Buck, and J.B. McGrory, Phys. Rev. Lett. **21**, 39 (1968).
[11] A.P. Zuker, Phys. Rev. Lett. **23**, 983 (1969).
[12] B.S. Reehal and B.H. Wildenthal, Part. Nucl. **6**, 137 (1973).
[13] G. Bertsch, J. Borisowicz, H. McManus, and W.G. Love, Nucl. Phys. **A284**, 399 (1977).
[14] J.P. Elliot, A.D. Jackson, H.A. Mavromatis, E.A. Sanderson, and B. Singh, Nucl. Phys. **A121**, 241 (1968).
[15] G.R. Satchler and W.G. Love, Phys. Rep. **55**, 123 (1979).
[16] F. Barranco, G.F. Bertsch, R.A. Broglia, and E. Vigezzi, Nucl. Phys. **A512**, 253 (1990).
[17] A. Arima and S. Yoshida, Nucl. Phys. **A219**, 475 (1974).
[18] F. Carstoiu, O. Dumitrescu, G. Stratan, and M. Braic, Nucl. Phys. **A441**, 221 (1985).
[19] M. Abramowitz and I. A. Stegun, *Handbook of Mathematical Functions* (National Bureau of Standards, Washington, DC, 1964).
[20] M. Ychimura, A. Arima, E.C. Halbert, and T. Terasawa, Nucl. Phys. **A204**, 225 (1973).
[21] H.R. Collard, L.R.B. Elton, and R. Hofstadter, *Kernradien* (Springer-Verlag, Berlin, 1967).
[22] D. Kurath and I.S. Towner, Nucl. Phys. **A222**, 1 (1974).
[23] Yu.F. Smirnov, Nucl. Phys. **27**, 177 (1961); **39**, 346 (1962).
[24] F. Ajzenberg-Selove, Nucl. Phys. **A460**, 1 (1986).
[25] B. Apagyi, G. Fai, and J. Nemeth, Nucl. Phys. **A272**, 303 (1976).
[26] J.B. McGrory and B.H. Wildenthal, Phys. Rev. C **7**, 974 (1973).